All-chalcogenide variable infrared filter

H. Esat Kondakci, Ozlem Koylu, Mecit Yaman, Aykutlu Dana, Mehmet Bayindir

H. Esat Kondakci, Ozlem Koylu, Mecit Yaman, Aykutlu Dana, Mehmet Bayindir, "All-chalcogenide variable infrared filter," Proc. SPIE 7419, Infrared Systems and Photoelectronic Technology IV, 74190A (27 August 2009); doi: 10.1117/12.825468

SPIE.

Event: SPIE Photonic Devices + Applications, 2009, San Diego, California, United States

All-chalcogenide variable infrared filter

H. Esat Kondakci[a,b], Ozlem Koylu[b], Mecit Yaman[b], Aykutlu Dana[b], and Mehmet Bayindir[a,b]

[a]Department of Physics, Bilkent University, 06800 Ankara, Turkey
[b]UNAM - Institute of Materials Science and Nanotechnology, Bilkent University, 06800 Ankara, Turkey

ABSTRACT

We present the design, fabrication, characterization of spatially variable infrared filter and a demonstration of the filter as a simple infrared spectrometer. A varying photonic band gap filter which consists of thermally evaporated, high refractive index contrast amorphous chalcogenide glass multilayers, makes the structure suitable to be used as spectrometer. Due to graded thickness structure, the filter exhibits a position dependent stop band and a cavity mode ranging from 2 to 8 μm wavelengths. It is demonstrated that the filter can be used to detect absorption peaks of common gases in the cavity mode range of the filter.

Keywords: Photonic crystals, omnidirectional photonic band gap, infrared filter, hand-held spectrometer

1. INTRODUCTION

Quarter wave stacks[1] (QWS) fabricated with high index contrast materials may posses full photonic band gaps resulting in omnidirectional reflection.[2,3] This opens up the possibility of making infrared (IR) mirrors[4] and filters[5–7] at specific wavelengths. By choosing suitable dielectric materials and controlling layer thicknesses, one can control the reflective and filtering characteristics. Such optical components can be used to design spectrometers, chemical and biological sensors at the IR region.[8]

The QWS structures can be fabricated by chemical vapor deposition,[9] sol-gel processing,[10] molecular beam epitaxy,[11] spin coating/thermal evaporation,[3] or only thermal evaporation.[12] In addition to above mentioned techniques, amorphous chalcogenide glasses can be thermally evaporated on large area polymer films.[13] In this case the radial QWS are obtained by rolling the coated polymer film on a cylindirical rod. Subsequently, the macroscopic structures are drawn into various photonic band gap fibers at visible[5,6] and IR wavelengths.[4] This study is motivated by the fact that chalcogenide glasses have unique properties such as high refractive indices and transparency at IR region. Therefore they are excellent materials in IR omnidirectional photonic applications.[6,14,15] Here we use omnidirectional mirrors-filter to design a simple IR spectrometer.

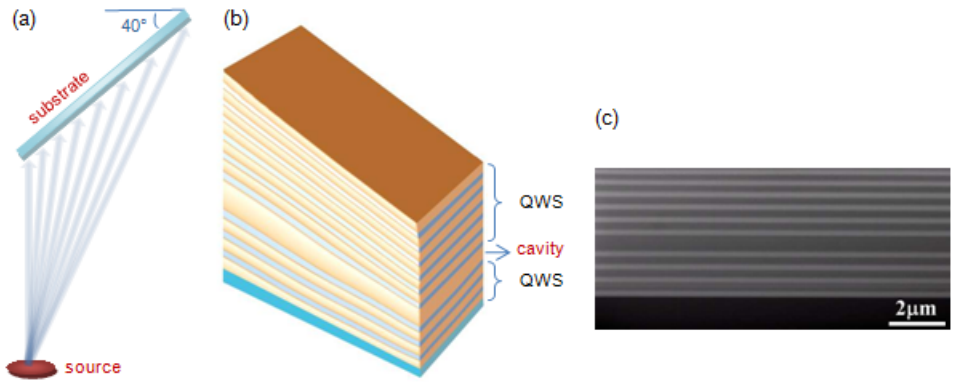

Figure 1. Schematic representation of (a) slanted evaporation geometry, (b) spatially variable multilayer filter structure and (c) cross sectional scanning electron micrograph of the 20 layer As_2S_3-$Ge_{15}As_{25}Se_{15}Te_{45}$ multilayer structure. The dark layers correspond to As_2S_3 layers with a $\lambda/2n$ cavity layer.

Infrared Systems and Photoelectronic Technology IV,
edited by Eustace L. Dereniak, John P. Hartke, Paul D. LeVan, Randolph E. Longshore, Ashok K. Sood,
Proc. of SPIE Vol. 7419, 74190A · © 2009 SPIE · CCC code: 0277-786X/09/$18 · doi: 10.1117/12.825468

2. FABRICATION

In QWS structures, position of the band depends on the thicknesses and refractive indices of dielectric layers. To gradually shift the position of the photonic band on a single substrate the thicknesses of the QWS should change monotonically from one side to the other. Thickness variation can be simply achieved by utilizing thermal evaporation onto an oblique surface from a point source.[16] To exploit this idea in order to fabricate a spatially variable IR filter, chalcogenide glasses are evaporated on a substrate with a slanted geometry as shown in Fig. 1(a,b).

Chalcogenide glasses were synthesised and their optical properties were characterized to be used as high index contrast materials. The high-index chalcogenide glass, $Ge_{15}As_{25}Se_{15}Te_{45}$ (GAST), was synthesized from high-purity (5-6N) Ge, As, Se, and Te elements (Alfa Aesar) using conventional sealed-ampoule melt-quenching techniques.[17,18] For the low-index material As_2S_3 (Amorphous Materials) was chosen due to thermal compatibility with GAST glass. To characterize optical properties of As_2S_3 and GAST thin films, bulk glasses were deposited on silicon substrates by thermal evaporation (Vaksis Elif, pressure $\sim 10^{-6}$ Torr, deposition rate $\sim$50 $\mathring{A}/s$).

The refractive index, n, and the extinction coefficients, k, of the deposited films are obtained in the visible, near-IR, and mid-IR region from spectroscopic ellipsometry measurements (J. A. Woollam Co., Inc. V-VASE, IR-VASE). As shown in Fig. 2, both chalcogenide glasses are transparent between 1.25 and 25 μm. At 3 μm, GAST and As_2S_3 have a high index ratio of 3.16:2.38, which is required for an omnidirectional photonic band gap.

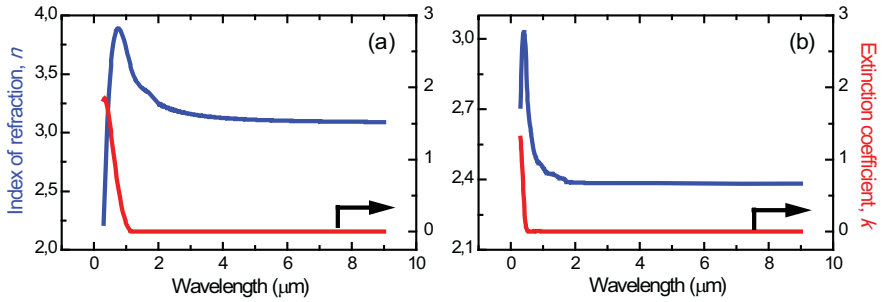

Figure 2. Measured index of refraction and extinction coefficient of (a) thermally evaporated $Ge_{15}As_{25}Se_{15}Te_{45}$ and (b) As_2S_3 thin films. The refractive index contrast allows to achieve omnidirectional photonic band gap.

As described above, the utilization of high index contrast chalcogenide glasses in a slanted geometry results in a position dependent full photonic band gap. Furthermore, doubling thickness layer in the middle of the multilayer structure results in a cavity mode within the photonic band gap. The cavity mode and photonic band gap of ten pairs of GAST and As_2S_3 layers with an As_2S_3 cavity layer (thirteenth layer from top) are simulated by using the generalized transfer matrix method for coherent and incoherent multilayer structures with finite substrates.[19] To further improve quality of the cavity mode of the filter and eliminate side bands a second filter is designed. In this case, 20 layer QWS of As_2S_3 and GAST with addition of $\lambda/8$ stacks on the top and bottom of the multilayers is simuleted with the same method. $\lambda/8$ stacks make possible to suppress the high frequency side band and placing the cavity layer eleventh layer from top gives rise to best quality factor of the cavity mode.

In accordance with the simulation results of the first design, ten pairs of alternating As_2S_3 and GAST layers are thermally evaporated with thicknesses, 315 and 237 nm, respectively, to produce a photonic stop band centered at 3 μm (Fig. 1(c)). The As_2S_3 cavity layer is located at the thirteenth layer from the top with a thickness of 630 nm. The graded thickness profile is obtained by simply giving a slant to the substrate with respect to the horizontal during thermal deposition as discussed earlier. In our case, a 40 degree slant gives a thickness profile for As_2S_3 (GAST) layer from 193 nm (140) to 365 nm (264) along the 5 cm substrate. The second filter is also similarly fabricated as described in the second design optimized for transmission measurements by using a double side polished silicon substrate.

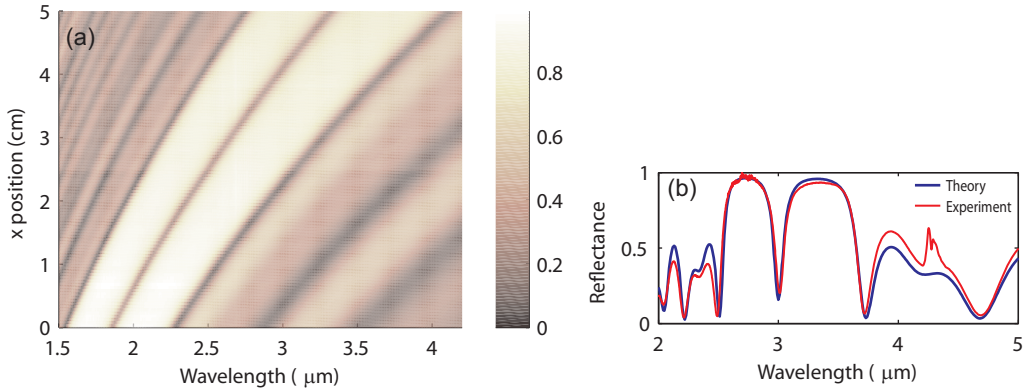

Figure 3. (a) Position dependent reflectance measurements taken from 80 linearly spaced positions along the sample.(b) Comparison of theoretical and experimental reflectance spectra taken at a position 4 cm away from the short-wavelength side of the filter. Both the simulation and FTIR measurements are performed at normal incidence.

3. RESULTS

In the fabrication part it is mentioned that the slanted evaporation geometry induces a graded thickness profile along the filters and cavity modes become position dependent. In order to determine the position dependence of the cavity mode of the first sample, Fourier transform infrared spectroscopy (FTIR) measurements in reflection mode are made along the substrate (Bruker FTIR Vertex 70 with Hyperion microscope). As shown in Fig. 3(a), the cavity mode shifts from 1.8 to 3.4 μm from one edge ($x = 0$) of the substrate to the other ($x = 5$ cm). The calculated reflection spectrum at 3 μm also agrees well with the measured results (Fig. 3(b)).

Furthermore the reflectance spectra of the filter are investigated for oblique angles by performing simulations for the cavity mode centered at 3 μm. Using the generalized transfer matrix method, the reflectance spectra are determined for all incidence angles and for both TE/TM polarizations. The omnidirectional reflections are also confirmed by the ellipsometric measurements at various incidence angles. Reflection spectra at three oblique angles are shown in Fig. 4 for both polarizations. The cavity mode is more sensitive to higher incidence angles to TM polarization.

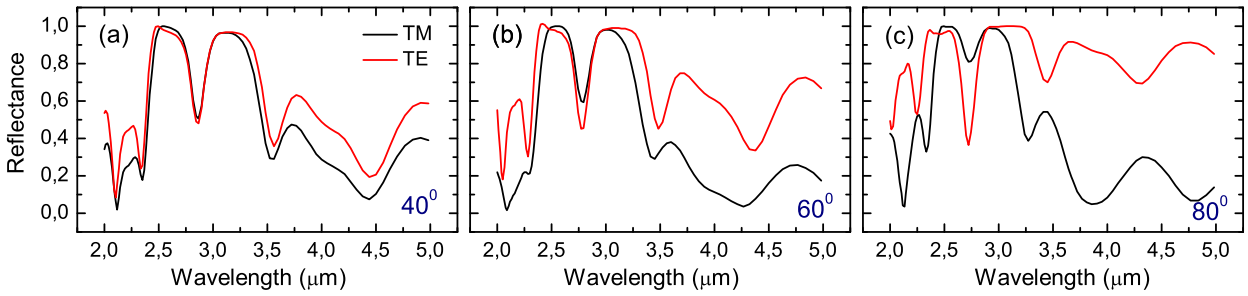

Figure 4. Measured reflectance spectra of the filter as a function of wavelength for (red lines) TE and (black lines) TM polarization modes at (a) 40°, (b) 60°, and (c) 80° angles of incidence.

The reflection spectra demonstrates that the peak wavelength of the cavity mode in the stop band is insensitive to angles of incidence. This makes the fabricated devices particularly suitable for IR spectral imaging and spectrometry applications. Using a hot filament as a source, even under poor collimation conditions, the filters effectively pass a narrow band of the IR radiation based on the spatial position.

We also fabricated the second filter sample according to the second design and we show the transmission profile of the filter obtained with the same FTIR system (Fig. 5). The transmission measurements show the

cavity mode shifts from 3.6 to 5.3 μm due to the graded thickness profile along the 2.5 cm part of the sample. Overall the sample, the cavity mode shifts from 2 to 8 μm on the 6 cm long filter.

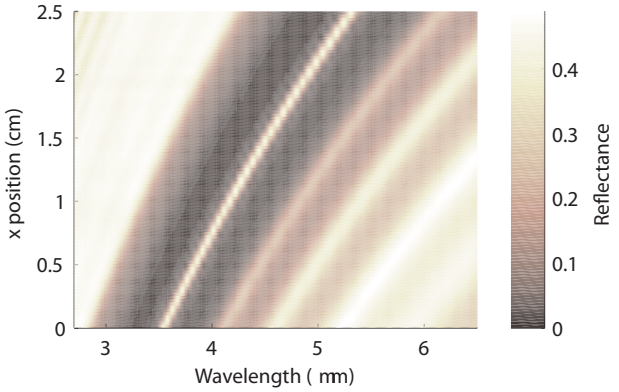

Figure 5. Position dependent transmittance measurements taken from 40 linearly spaced positions along the 3 cm part of the sample.

Next we present a demonstration of the filter as a simple IR spectrometer using the taken transmission spectra of the second filter. The spectrometer consists of a a hot filament as a blackbody source, the filter and an IR detector assuming that measures the integrated intensity of the signal within the range 4-10 μm. The schematic illustration of the spectrometer is shown in Fig. 6.

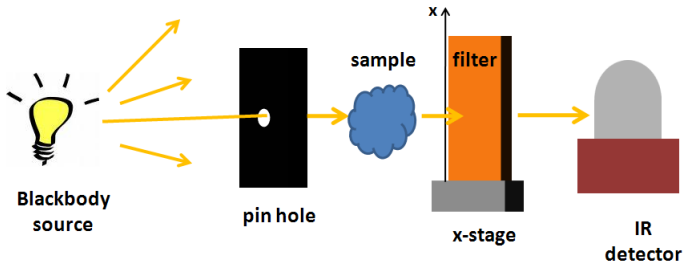

Figure 6. Schematic illustration of the spectrometer's experimental setup.

In order to simulate spectrometer, a black body source at 600 K and simplified transmission spectrum of CO_2 gas molecules are generated as in vacuum conditions (Fig. 7). Then, by multiplying the black body source with the transmission spectrum and integrating spectra between the IR detector range to get intensity for each x-position on the filter, we generate intensity spectrum with respect to x-position of the filter.

The intensity signal at the x-position of the filter can be formulated as

$$I_{BG,x}(\omega_{c,x}) = \int_{\omega_1}^{\omega_2} I_{BB}(\omega) * T_x(\omega) d\omega \tag{1}$$

where $I_{BG,x}(\omega_{c,x})$ is the intensity of the background signal at the x-position, $I_{BB}(\omega)$ is the spectral intensity of the blackbody radiation and $T_x(\omega)$ is the transmittance spectrum of the spectrometer at the x-position which corresponds to a specific cavity mode of angular frequency $\omega_{c,x}$. Then assuming CO_2 gas sample is placed between the blackbody source and the filter, we similarly generate intensity spectrum. In the presence of the gas sample the intensity signal at the x-position of the filter can be formulated as

$$I_x(\omega_{c,x}) = \int_{\omega_1}^{\omega_2} I_{BB}(\omega) * T_M(\omega) * T_x(\omega) d\omega \tag{2}$$

where $T_M(\omega)$ is the transmission spectrum of the gas sample. In Fig. 8 multiplications of the black body source and transmission spectra of the filter with the absence (blue straight lines) and presence (red dotted lines) of CO_2 gas molecules is shown for three different x-positions which correspond to (a) 3.61 μm, (b) 4.26 μm, and (c) 5.32 μm. Intensity spectrum with respect to x-position of the filter is shown in Fig. 8(d). The difference of the intensities and derivative of that imply where the absorption peak of the gas sample is located (Fig. 8(e,f)).

A resistive wire was heated and emitted IR radiation was collimated using two pinholes. The collimated beam was then passed through the 3 cm long gas chamber. The background measurements are done using N_2 and CO_2 gas was used as the sample gas. The signal was detected using a standard thermopile with the help of a lock-in amplifier and a mechanical chopper (Stanford Research Systems SR830) to reduce noise. The filter was positioned between the detector and the sample stage and shifted perpendicularly using a Newport ESP300 3-axis stage controller with a resolution of 0.5 mm along 2.5 cm part of the filter. 0 cm x-position of the filter corresponds to cavity mode at 3.61 μm and 2.5 cm x-position corresponds to 5.32 μm. In Fig. 9, measured

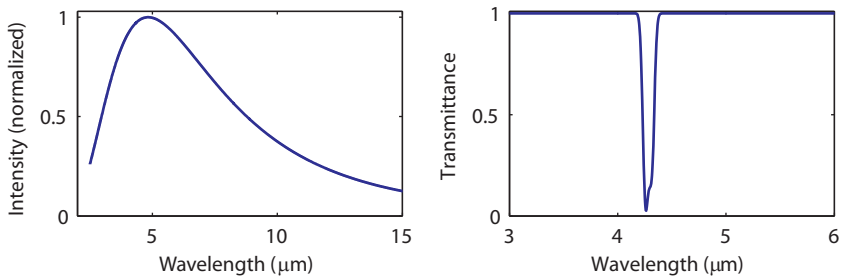

Figure 7. (a) Black body radiation spectrum of a resistive wire at 600 K. (b) Simulation of simplified transmission spectrum of an CO_2 gas molecules

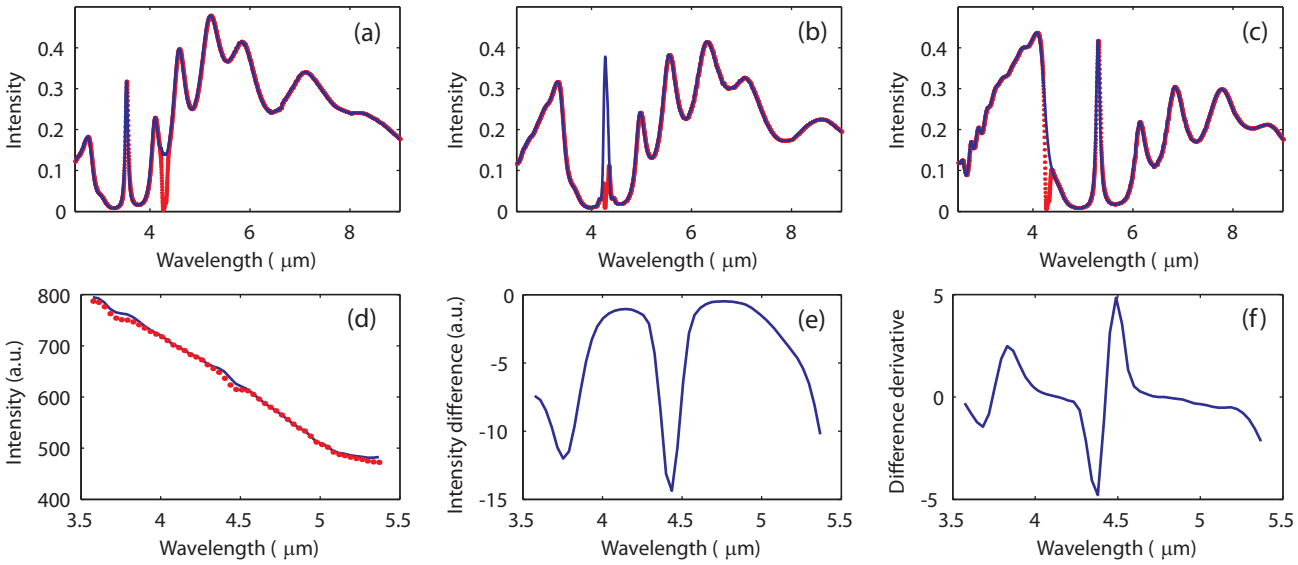

Figure 8. The transmittance spectrum of the blackbody radiation through IR filter with (CO_2) and without (N_2) the sample for three spatial positions corresponding to the cavity modes (A) 3.61 (B) 4.25 (c) 5.32. (d) The simulation of the integrated intensities of the detector. (e) The difference of the integrated signals showing the CO_2 absoprtion peak at 4.25. (f) The derivative of the difference signal further highlights the absorption peak.

position dependent intensities and the difference of that are shown. Around the 12 mm x-position, there is a decrease in intensity which corresponds to 4.28 μm in calibrated scale. The decrease in the intensity implies absorption peak of the CO_2 absoprtion peak.

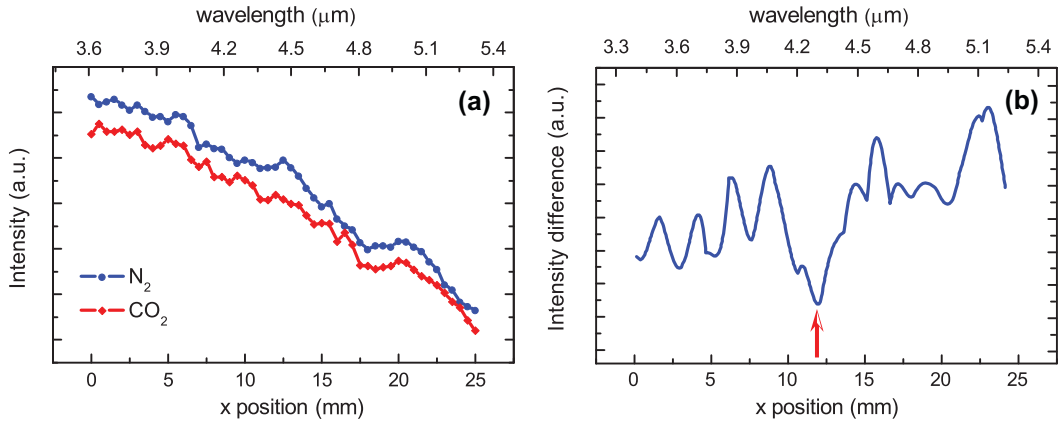

Figure 9. (a)The measured intensities with (CO_2) and without (N_2) using the thermopile detector. (b)The difference of the integrated signals showing the CO_2 absoprtion peak at 4.25μm.

4. CONCLUSION

We have successfully demonstrated an IR spectrometer made with a position dependent omnidirectional photonic band gap filter. The filter is fabricated by thermal evaporation of IR transparent chalcogenide glasses on a silicon substrate. The simple design and fabrication with relatively inexpensive components made possible the realization of a portable IR spectrometer that can effectively be used to detect absorption lines of gaseous samples in the IR spectrum. The spectrometer can easily be improved to operate as a full-fledged IR spectrometer with improved electronics.

REFERENCES

[1] P. Yeh, A. Y. and Hong, C.-S., "Electromagnetic propagation in periodic stratified media. i. general theory," *J. Opt. Soc. Am.* **67**, 423–437 (1977).

[2] Winn, J., Fink, Y., Fan, S., and Joannopoulos, J., "Omnidirectional reflection from a one-dimensional photonic crystal," *Opt. Lett.* **23**(20), 1573–1575 (1998).

[3] Fink, Y., Winn, J., Fan, S., Chen, C., Michel, J., Joannopoulos, J., and Thomas, E., "A dielectric omnidirectional reflector," *Science* **282**(5394), 1679–1682 (1998).

[4] Temelkuran, B., Hart, S., Benoit, G., Joannopoulos, J., and Fink, Y., "Wavelength-scalable hollow optical fibres with large photonic bandgaps for CO2 laser transmission," *Nature* **420**(6916), 650–653 (2002).

[5] Bayindir, M., Sorin, F., Abouraddy, A., Viens, J., Hart, S., Joannopoulos, J., and Fink, Y., "Metal-insulator-semiconductor optoelectronic fibres," *Nature* **431**(7010), 826–829 (2004).

[6] Abouraddy, A. F., Bayindir, M., Benoit, G., Hart, S. D., Kuriki, K., Orf, N., Shapira, O., Sorin, F., Temelkuran, B., and Fink, Y., "Towards multimaterial multifunctional fibres that see, hear, sense and communicate," *Nature Mat.* **6**(5), 336–347 (2007).

[7] Bayindir, M., Abouraddy, A. F., Shapira, O., Viens, J., Saygin-Hinczewski, D., Sorin, F., Arnold, J., Joannopoulos, J. D., and Fink, Y., "Kilometer-long ordered nanophotonic devices by preform-to-fiber fabrication," *IEEE J. Sel. Top. Quantum Electron.* **12**(6, Part 1), 1202–1213 (2006).

[8] Sanghera, J., Shaw, L., and Aggarwal, I., "Applications of chalcogenide glass optical fibers," *C. R. Chimie* **5**(12), 873–883 (2002).

[9] Carlin, J., Zellweger, C., Dorsaz, J., Nicolay, S., Christmann, G., Feltin, E., Butte, R., and Grandjean, N., "Progresses in III-nitride distributed Bragg reflectors and microcavities using AlInN/GaN materials," *Phys. Stat. Sol. B* **242**(11), 2326–2344 (2005).

[10] Almeida, R. and Rodrigues, A., "Photonic bandgap materials and structures by sol-gel processing," *J. Non-Cryst. Solids* **326**, 405–409 (2003).

[11] Baumgartner, E. W., Schwarzl, T., Springholz, G., and Heiss, W., "Highly efficient epitaxial Bragg mirrors with broad omnidirectional reflectance bands in the midinfrared," *Appl. Phys. Lett.* **89**(5), 051110 (2006).

[12] Kohoutek, T., Orava, J., Wagner, T., Hrdlicka, M., Vlcek, M., and Frurnar, M., "Preparation of dielectric mirrors from high-refractive index contrast amorphous chalcogenide films," *J. Phys. and Chem. Solids* **69**(8), 2070–2074 (2008).

[13] Hart, S., Maskaly, G., Temelkuran, B., Prideaux, P., Joannopoulos, J., and Fink, Y., "External reflection from omnidirectional dielectric mirror fibers," *Science* **296**(5567), 510–513 (2002).

[14] Zakery, A. and Elliott, S., "Optical properties and applications of chalcogenide glasses: a review," *J. Non-Cryst. Solids* **330**(1-3), 1–12 (2003).

[15] Bureau, B., Zhang, X., Smektala, F., Adam, J., Troles, J., Ma, H., Boussard-Pledel, C., Lucas, J., Lucas, P., Le Coq, D., Riley, M., and Simmons, J., "Recent advances in chalcogenide glasses," *J. Non-Cryst. Solids* **345**, 276–283 (2004).

[16] Kondakci, H. E., Yaman, M., Koylu, O., Dana, A., and Bayindir, M., "All-chalcogenide glass omnidirectional photonic band gap variable infrared filters," *Appl. Phys. Lett.* **94**(11), 111110 (2009).

[17] Bayindir, M., Shapira, O., Saygin-Hinczewski, D., viens, J., Abouraddy, A., Joannopoulos, J., and Fink, Y., "Integrated fibres for self-monitored optical transport," *Nature Mat.* **4**(11), 820–825 (2005).

[18] Bayindir, M., Abouraddy, A., Arnold, J., Joannopoulos, J., and Fink, Y., "Thermal-sensing fiber devices by multimaterial codrawing," *Adv. Mat.* **18**(7), 845 (2006).

[19] Katsidis, C. and Siapkas, D., "General transfer-matrix method for optical multilayer systems with coherent, partially coherent, and incoherent interference," *App. Opt.* **41**(19), 3978–3987 (2002).